SPACE TELESCOPE SCIENCE INSTITUTE
Operated for NASA by AURA

Instrument Science Report WFC 2014-12

Astrometric Correction for WFC3/UVIS Filter-Dependent Component of Distortion

V. Kozhurina-Platais

May 27, 2014

Abstract

Observations of the central field in ω Cen taken with large dither patterns and over a large range of HST roll-angles, exposed through 14 UVIS filter, have been used to examine the astrometric irregularities in the WFC3/UVIS filters. These irregularities introduce fine-scale astrometric errors at the level of about 0.1 pixel with a complicated spatial structure across the WFC3/UVIS CCD chips. The fine-scale solution was utilized to construct a 2–D look-up table for each of the 14 WFC3/UVIS filter in order to account for the filter-dependent component of distortion. The derived 2–D look-up tables can be interpolated at any point in the WFC3/UVIS image by STDAS software DrizzlePac/AstroDrizzle. The main results of this calibration are: 1) new polynomial coefficients of geometric distortion for 14 calibrated UVIS filters in the form of Instrument Distortion Correction Table (IDCTAB file) are improved to account for the lithographic-mask pattern in the WFC3/UVIS detector and filter-dependent distortion; 2) new look-up tables in the form of a D2IMFILE and NPOLFILEs significantly improve by 50-90% (depending on the filter) the fine-scale structure in the WFC3/UVIS geometric distortion; 3) new improved IDCTAB coupled with the D2IMFILE & NPOLFILEs can now successfully correct the astrometric errors down to the precision level of ∼ 0.02 UVIS pixel (or ∼1mas).

1. Introduction

An accurate model of geometric distortion for any HST imaging instrument is a backbone of the STSDAS software Multidrizzle (Fruchter & Hook, 2002, Koekemoer, 2002, and Fruchter & Sosey *et al.*, 2009) and the recently improved *DrizzlePac/Astrodrizzle* software (Gonzaga, *et al.*, 2012), which is currently installed in the STScI on-the-fly pipeline (OTFR). This software requires accurate distortion correction in order to combine dithered HST images, and, thus, enhance the spatial resolution and deepen the detection limit. If the geometric distortion correction, implemented in *DrizzlePac* is not sufficiently accurate, then the HST image-combination process can produce blurred images and distort the under-sampled Point Spread Function (PSF).

In addition to geometric geometric distortion (*large-scale distortion*), which can be modeled with a high order polynomial (3rd or higher) and, which is due to the optical assembly of HST, there is a *micro-distortion*, which consists of fine-scale systematics in the residuals from the best-fit polynomial solutions. These fine-scale systematic residuals typically extend to ∼0.15 pixel and vary in amplitude depending on the location within a CCD chip. Such residuals cannot be removed by a polynomial model. These fine–scale and low–amplitude distortions are the result of: 1) a detector flaw caused by the manufacturing process and 2) imperfections of the individual filters them-self. For example, in the case of WFPC2, a small manufacturing defect occurs at every ∼ 34th row of each of the WFPC2 chips (Anderson & King, 1999). This defect introduced errors in photometry at the level of 0.01-0.02 magnitude, and periodic errors in astrometry at about the ∼0.03 pixel level. In the case of the ACS/WFC, a similar detector defect was identified in every ∼68th column for each of the WFC CCD chips, which induces a periodic error in astrometry of ∼0.1-0.8% (Anderson, 2002). For both WFPC2 and ACS/WFC, the detector defect is a 1–D correction, in either the X or Y direction. Recently, it was found that the ACS/WFC detector is affected by significant pixel grid irregularities in both ACS/WFC1 CCD chips, which can reach at ∼0.2 ACS pixels in amplitude across the ACS/WFC FOV (ACS-ISR, Kozhurina-Platais *et al*, in preparation). A complicated and correlated structure of residuals is similar in other ACS/WFC filters, which is an indication that irregularities in the pixel grid in the detector due to manufacturing process of ACS/WFC CCD. The origin of this effect is not yet well understood (D.Golimowski & M. Sirianni).

In the case of WFC3/UVIS, the pixel–grid irregularities are due to the lithographic-mask pattern is imprinted onto the detector itself (Kozhurina-Platais, *et al*, 2010, 2013). The complicated structure of the irregularities in the pixel–grid cannot be modeled by high–order polynomial. A simple way to remove a complicated and fine-scale variations in X & Y raw positions across of the CCD detector is to construct a look-up table, which then can be linearly interpolated at any point in the WFC3/UVIS images, prior to the large-scale distortion (polynomial model) correction. The WFC3/UVIS lithographic pattern is also described by Bellini *et al.*, (2011), although in that work, the detector defect (lithographic-

pattern mask correction) has not been separated from fine-scale distortion in the filter itself. However, the detector defect is filter *independent* and therefore it should always be applied to the X & Y UVIS raw positions first, prior to correction of geometric distortion and its filter-dependent component of distortion.

As described in Kozhurina-Platais *et al* (2013), the WFC3/UVIS lithographic pattern correction was designed for specific use in STSDAS software *DrizzlePac/Astrodrizzle* (Gonzaga, *et al*, 2012) and for use in the STScI on-the-fly pipeline and OPUS. The constructed 2D look-up table correction, in the form of reference file *D2IMFILE*, should be in a specific format complying with specifications imposed by *DrizzlePac/Astrodrizzle*. After applying the geometric distortion correction coupled with the lithographic-mask pattern correction, the astrometric errors in the WFC3/UVIS drizzled images were improved, nevertheless, there are some remaining small correlated offsets at the boundary of each lithographic-mask pattern up to 0.05 pixel. These remaining offsets introduce additional systematics in each set of filter-dependent distortion corrections. Therefore, before deriving filter-dependent distortion, unaccounted errors for lithographic-mask patterns should be reduced.

Here, we present the analysis and results of the improved lithographic-mask pattern correction in the WFC3/UVIS X,Y raw positions, and UVIS filter-dependent distortion coupled with improved geometric distortion polynomial coefficients.

2. Correction for the WFC3/UVIS Distortions

2.1. WFC3/UVIS Lithographic-Mask Patterns and Its Correction

In previously work by Kozhurina-Platais *et al.*, (2013), the averaged vector of residuals between UVIS positions and the reference catalog after the best polynomial fit, have been smoothed in the bin size of 128×128 pixels. In order to improve the correction for lithographic-mask patterns, instead of using the averaged vector of residuals in the bin size of 128×128 pixels, we adopted the technique from Anderson & King (2004) used for the fine-scale structure correction in ACS/WFC and ACS/HRC wide-band filters, by smoothing the residuals in the bin size of 65×65 pixels. Following by this approach, a 65×65-pixel bin size have been imposed over the entire 4096×2051 pixel residual map of each UVIS CCD chip. The numerical implementation was realized in the FORTRAN code which involves binning residuals over an array of 64×32 points and then smoothing them. The binned data are first averaged with iterative sigma-clipping. Then, each grid point of residuals is smoothed with a 5×5 quadratic kernel (Anderson & King, 2000). The resulting smoothed map of residuals between the positions in F606W filter and the standard astrometric catalog after removing the geometric distortion is shown in Figure 1. As can be seen, the lithographic-mask boundaries have been smoothed out with an array of 64×32 points, whereas the lithographic-mask patterns are an array of 6×2 zones with the size of ∼700×1000 pixels. A small bin-size of 65×65-pixel is chosen to accommodate the format limitations which comply with the

constrains of software *Drizzles/AstroDrizzle/TweakReg* and the STScI on-the-fly pipe-line (OTFR).

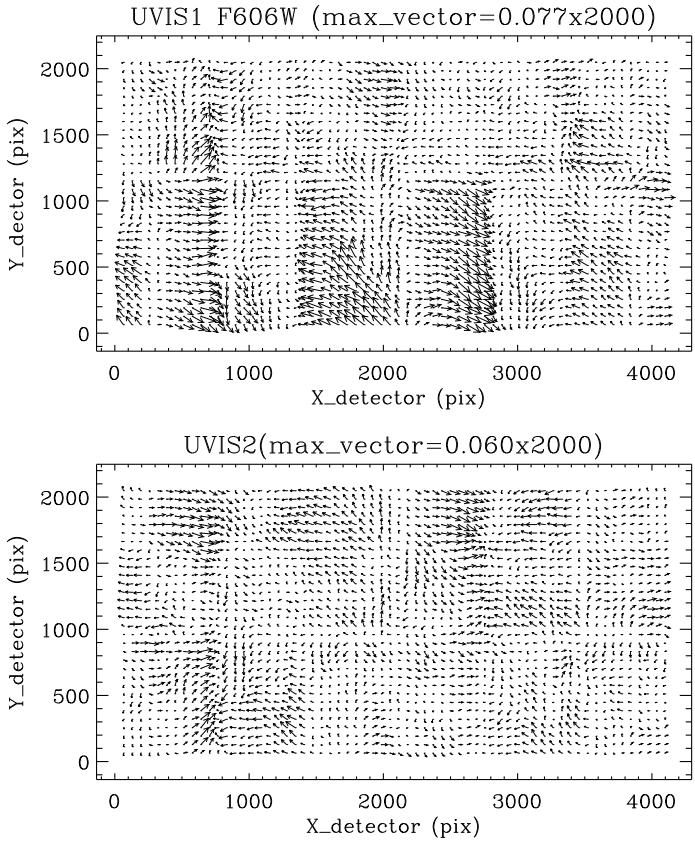

Fig. 1.— Vector diagram showing the smoothed residuals over an array of 64×32 points. The vector diagram have shown the smoothed boundaries of the WFC3/UVIS lithographic-mask patterns with period ∼675 pixels in X direction and 911 & 1140 pixels in the Y direction, symmetrically with respect to the gap between the two UVIS CCD chips. The top panel shows the X and Y residuals for the WFC3/UVIS1 CCD chip and the bottom panel X and Y residuals for WFC3/UVIS2 CCD chip. The largest vector (max_vector) is defined for both UVIS CCD chips, and both magnified by a factor of 2000. The units are WFC3/UVIS pixels.

Applying the derived look-up table of lithographic-mask patterns correction to the raw X and Y positions, and then correcting for the new improved polynomial coefficients of geometric distortion, the vectoring plot of residuals in F606W filters look essential free of any systematics (Figure 2). As can be seen, there is no indication of the lithographic-mask pattern and any spatial structure. The residual map looks smooth, the noise is reduced down to ∼0.01 pixels.

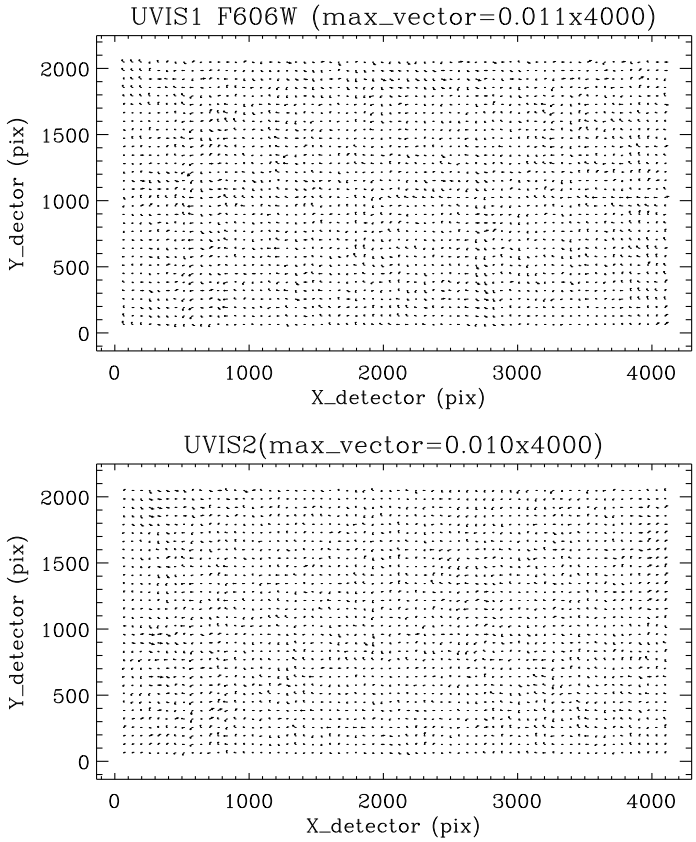

Fig. 2.— The same as in Figure 1, but after the correction for lithographic-mask pattern and using an improved geometric distortion coefficients. The largest vector ∼0.01 pixel, and magnified by a factor of 4000. The units are WFC3/UVIS pixels.

It is also necessary to mention here, that F606W has less structure in the residuals map compare to the residuals maps for other UVIS filters, as is shown by Figure 3 in Kozhurina-Platais *et al.*, (2013), which is an indication of small irregularities due to manufacture of the filter itself. Consequently, the resulting look-up table correction derived from observations taken through the F606W filter was used to correct the X and Y raw positions for the WFC3/UVIS lithographic-mask pattern in each of the 14 calibrated UVIS filters. Since this new correction is applied to all 14 calibrated filters, the new geometric distortion solution

for each of these filters was generated, yielding a new improved polynomial coefficients of the UVIS geometric distortion in the form of IDCTAB.

This 2–D look-up table correction has been implemented in PyWCS and STWCS (Python/PyRaf tasks) and converted into the FITS format as a reference file to be used in STSDAS software *DrizzlePac/Astrodrizzle* and in the STScI on-the-fly pipeline (OTFR). The keyword for this correction is D2IMFILE in the primary header of WFC3/UVIS images.

Thus, in the software *DrizzlePac/Astrodrizzle*, the reference file D2IMFILE, representing the lithographic-mask patterns correction is bi-linearly interpolated and used for pixel-by-pixel correction prior to correction for geometric distortion *via* polynomial coefficients.

2.2. WFC3/UVIS Filter–Dependent–Distortion

After applying the correction for lithographic-mask patterns to X & Y raw positions, the residuals map between UVIS positions and reference catalog after the best polynomial fit show a complicated fine-scale structure of systematic errors across both UVIS CCD chips. The amplitude of residuals varies from $\sim$0.05 to $\sim$0.1 UVIS pixels and the fine-scale residuals are different for different filters. The complicated structure in X & Y residuals with variations from filter to filter is the indication of the filter-dependent component of distortion due to their manufacturing process. The complicated structure of residuals after applying the correction for the WFC3/UVIS lithographic-mask patterns and the best-fit polynomial can be modeled by a high–order polynomial, but it would be inconvenient and complicated. To remove it, the smoothing technique as described in above (Para 2.1) was used again to obtain a 2–D look-up table correction for each calibrated UVIS filter. The resulting smoothed maps of filter-dependent correction for each filters are shown in Figures 3-16 (left panels).

An iterative process is required to improve the filter-dependent distortion correction and simultaneously improve the polynomial coefficients of geometric distortion. As a result, the systematic errors in the residual are reduced from $\sim$0.1 pixel down to $\sim$ 0.02 pixel, depending on the filter. Figures 3-16 show 2–D X & Y map of residuals between positions in each UVIS filters (after the lithographic-mask patterns, filter-dependent distortion & improved polynomial geometric distortion corrections) and the standard catalog. For example, Figure 14 shows some of the largest filter-dependent systematics in the residuals map and indicates that such systematic errors can be removed to a negligible level.

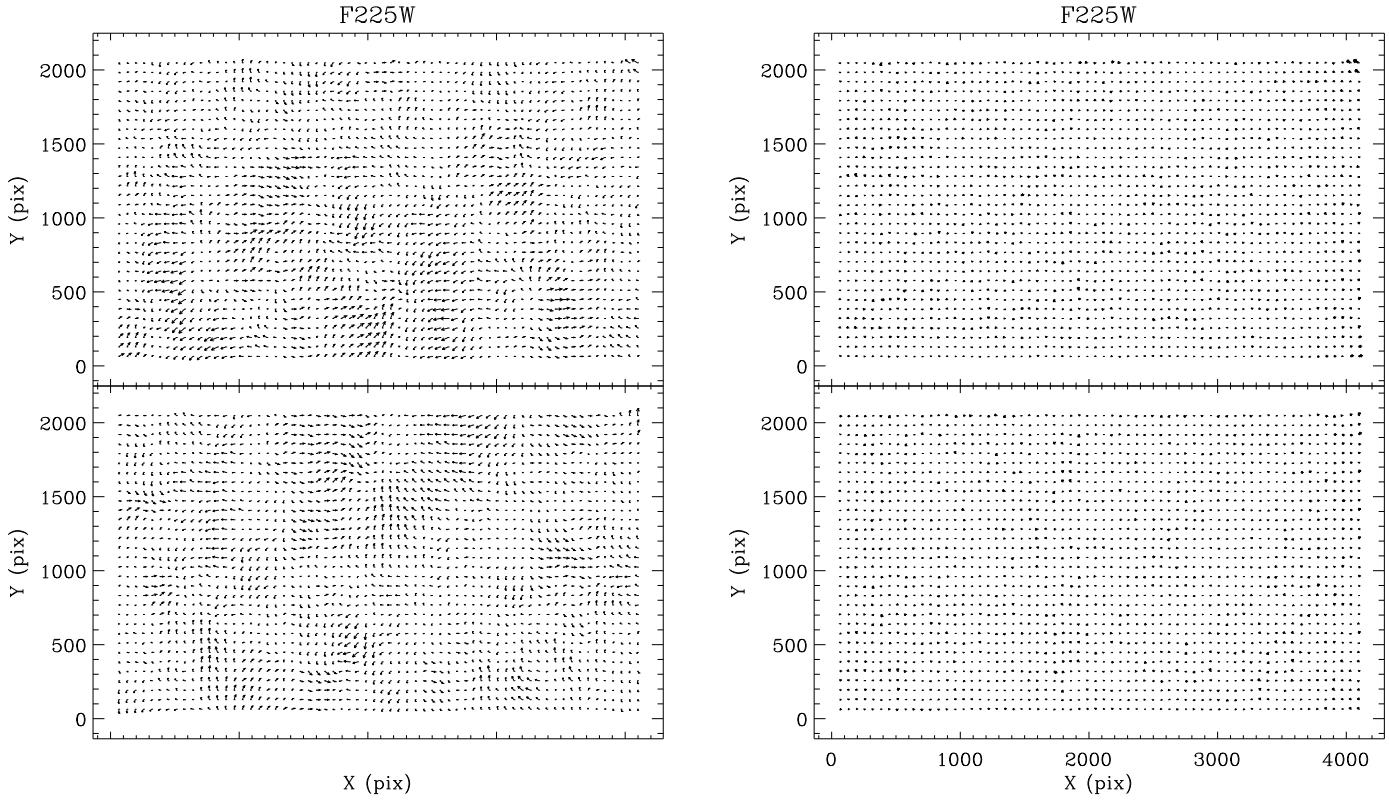

Fig. 3.— *Left panel:* 2-D X and Y residual map between positions in UVIS F225W filter and the standard catalog after the polynomial geometric distortion and lithographic-mask pattern are removed. The top panel shows the X and Y residuals for the WFC3/UVIS1 CCD chip and the bottom panel X and Y residuals for WFC3/UVIS2 CCD chip. The largest vector is ∼0.036 pixel. *Right panel:* the same as on the left but after the correction for UVIS F225W filter-dependent distortion. The largest vector is ∼0.015 pixel, magnified by a factor of 2000. The units are WFC3/UVIS pixels.

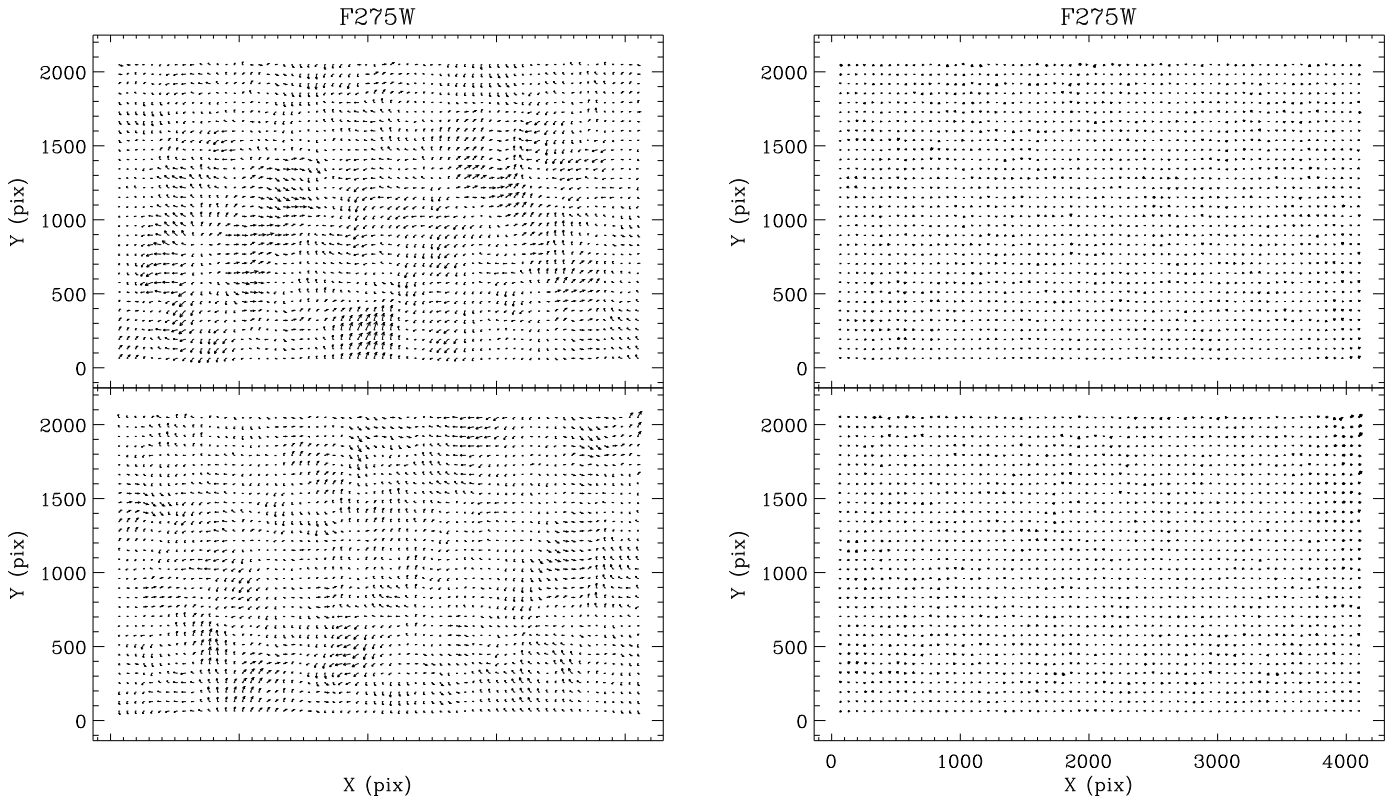

Fig. 4.— The same as Fig.3, only for the F275W UVIS filter. The largest vector before corrections is ∼0.038 pixel, and 0.016 pixel after the correction, both magnified by a factor of 2000. The units are WFC3/UVIS pixels.

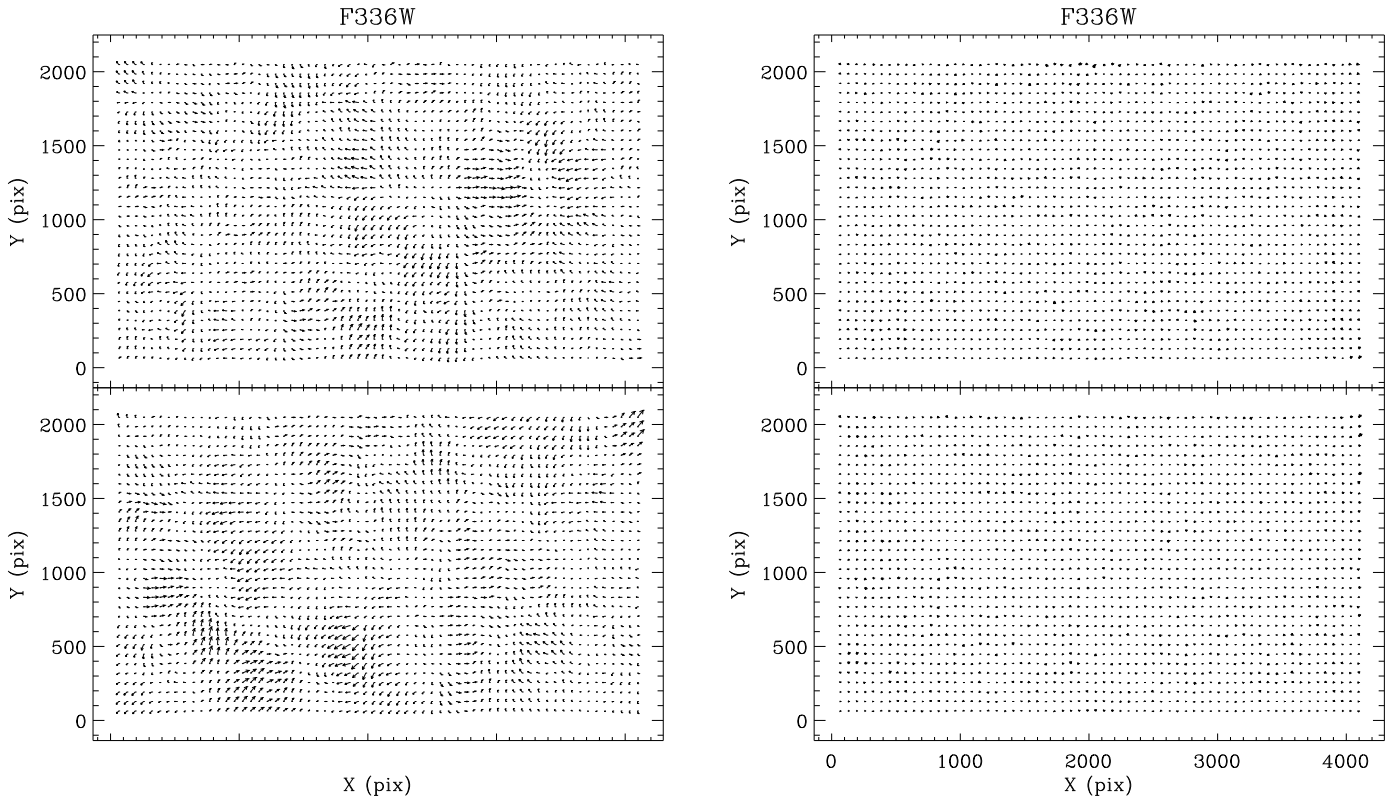

Fig. 5.— The same as in Fig.3, but for F336W UVIS filter. The largest vector before correction is ∼0.038 pixel, and 0.012 pixel after correction, both magnified by a factor of 2000. The units are WFC3/UVIS pixels.

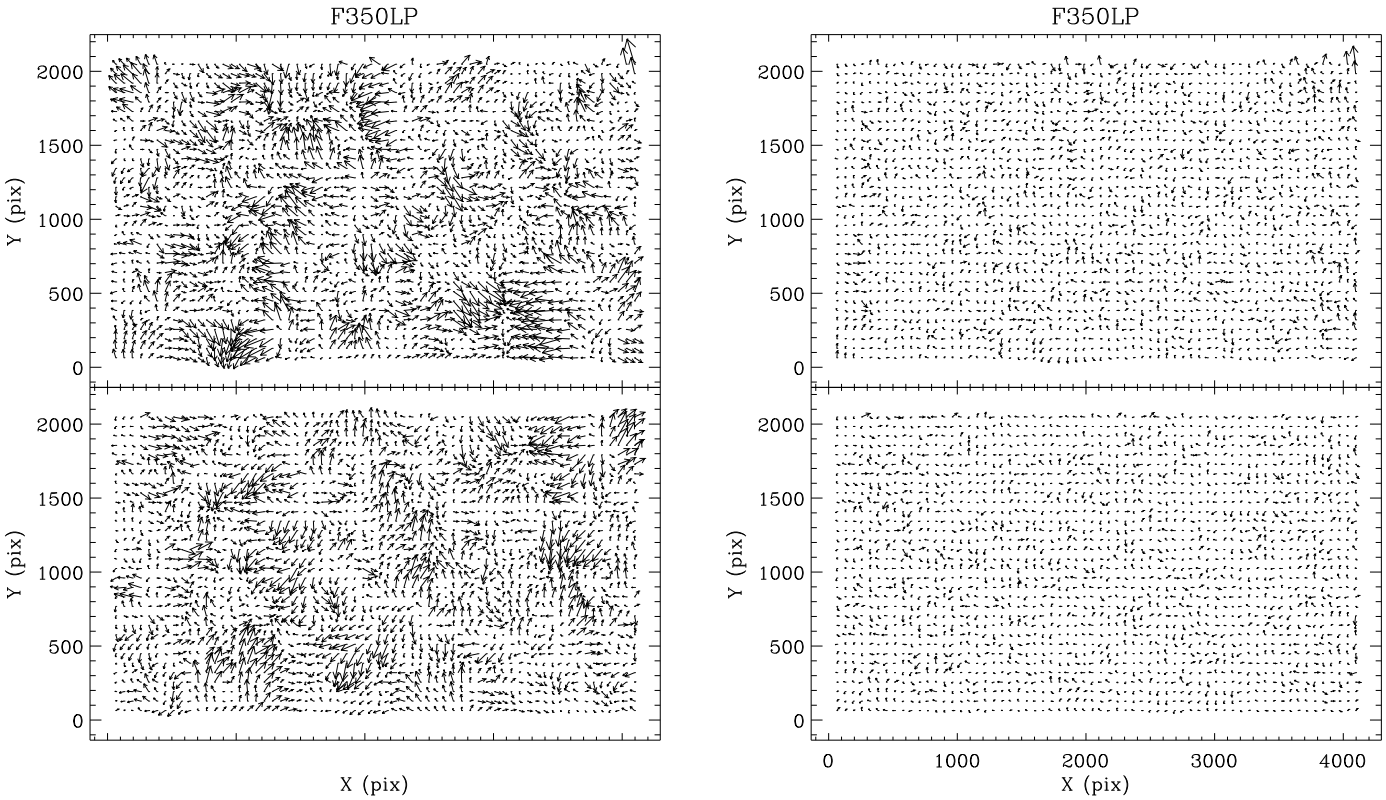

Fig. 6.— The same as in Fig.3, but for F350LP UVIS filter. The largest vector before correction is ∼0.117 pixel, and 0.068 pixel after the correction , both magnified by a factor of 2000. The units are WFC3/UVIS pixels. Insufficient number of observations in F350LP filter may explain noisy in the residuals after the correction for F350LP filter-dependent distortion.

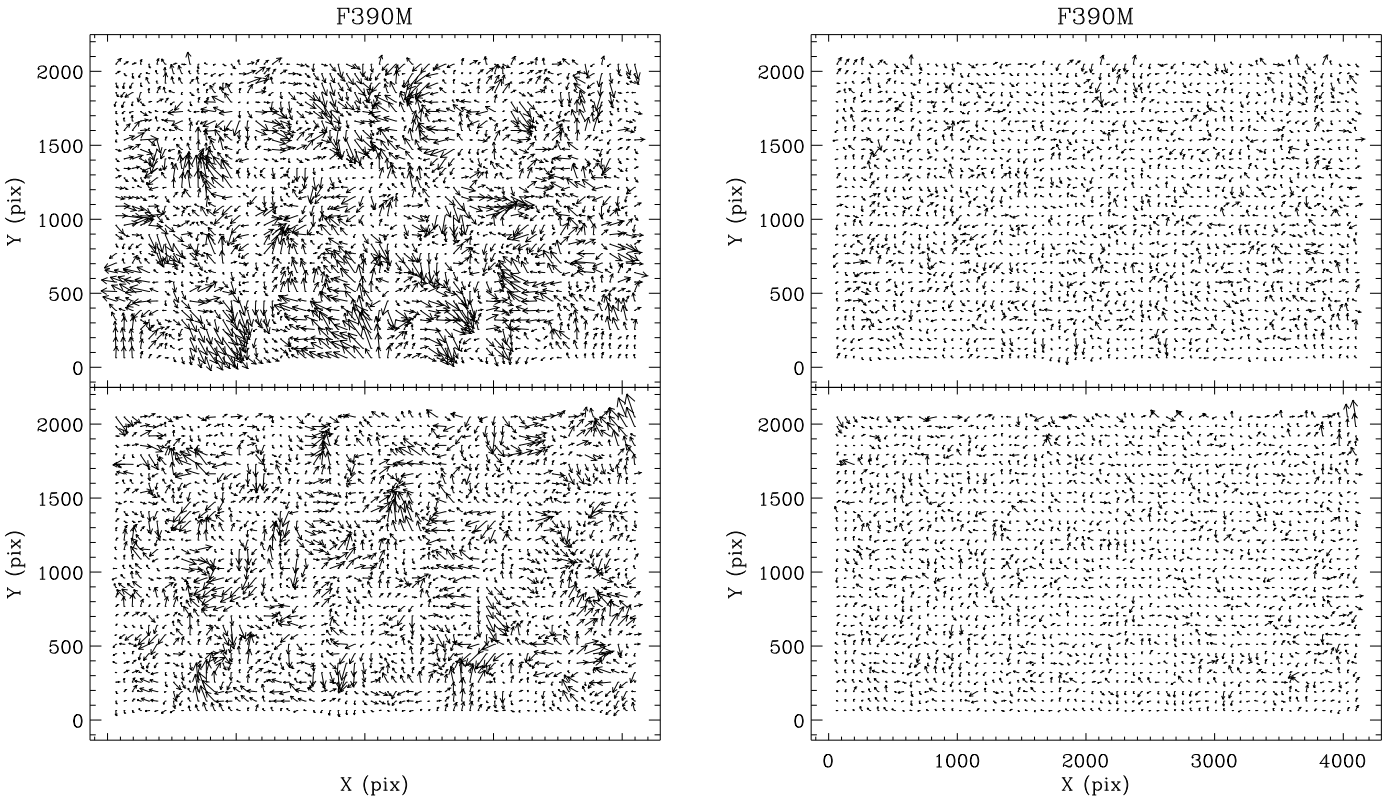

Fig. 7.— The same as in Fig.3, but for F390M UVIS filter. The largest vector before correction is ∼0.127 pixel, and 0.066 pixel after the correction , both magnified by a factor of 2000. The units are WFC3/UVIS pixels. Insufficient number of observations in F390M filter may explain noisy in the residuals after the correction for F390M filter-dependent distortion.

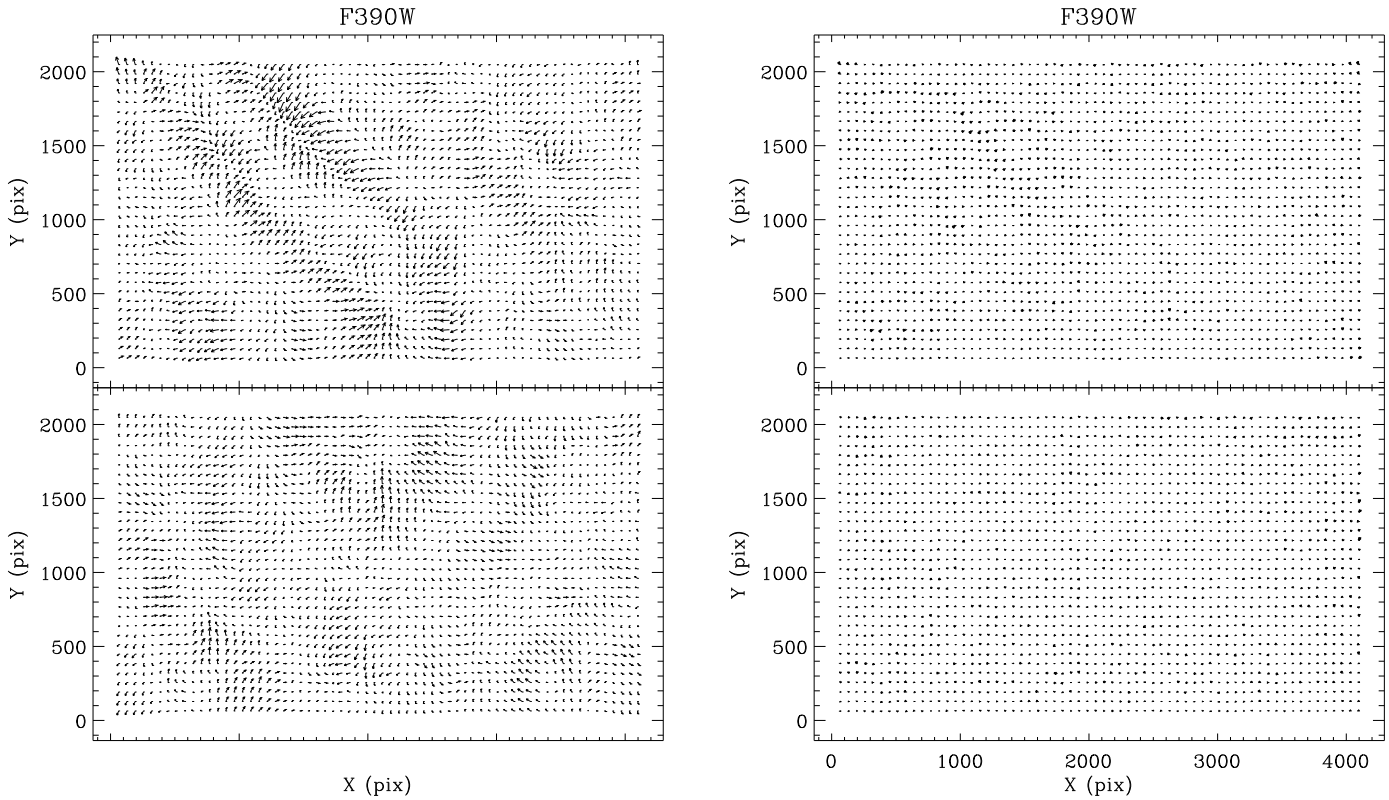

Fig. 8.— The same as in Fig.3, but for F390W UVIS filter. The largest vector before correction is ∼0.040 pixel, and 0.012 pixel after the correction , both magnified by a factor of 2000. The units are WFC3/UVIS pixels.

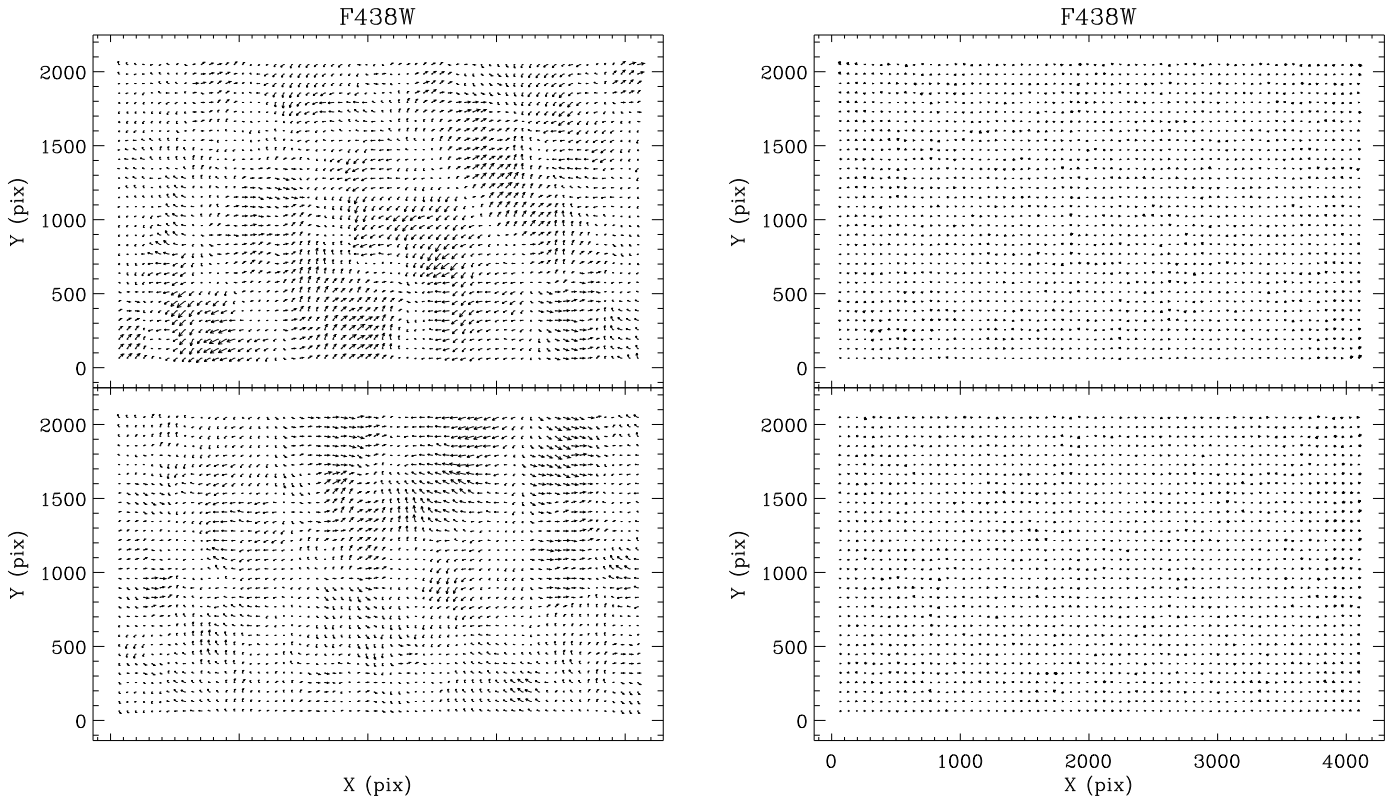

Fig. 9.— The same as in Fig.3, but for F438W UVIS filter. The largest vector before correction is ∼0.035 pixel, and 0.012 pixel after the correction , both magnified by a factor of 2000. The units are WFC3/UVIS pixels.

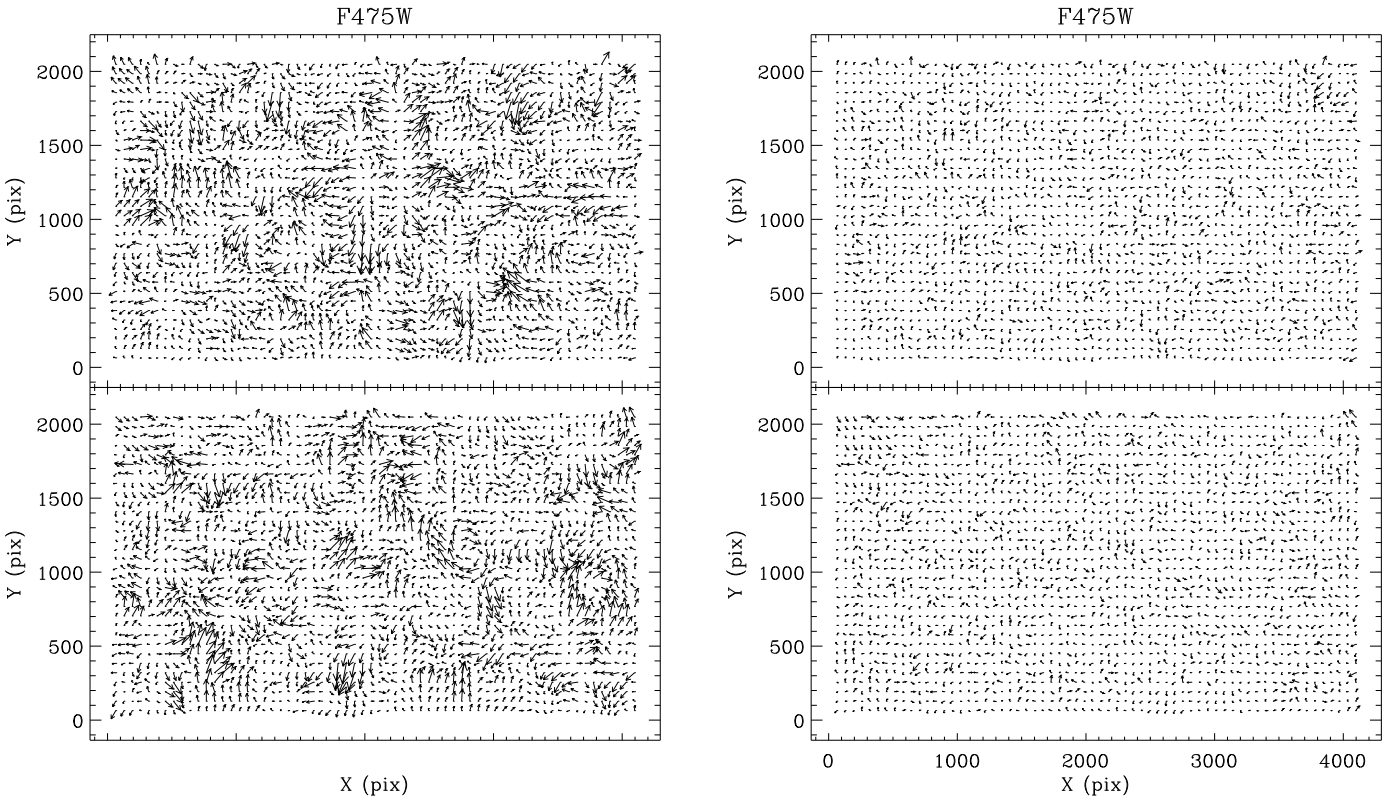

Fig. 10.— The same as in Fig.3, but for F475W UVIS filter. The largest vector before correction is ∼0.085, and 0.042 pixel after correction, both magnified by a factor of 2000. The units are WFC3/UVIS pixels. Noticeable noise in the residual map before and after the correction, can be due to the insufficient number of observations.

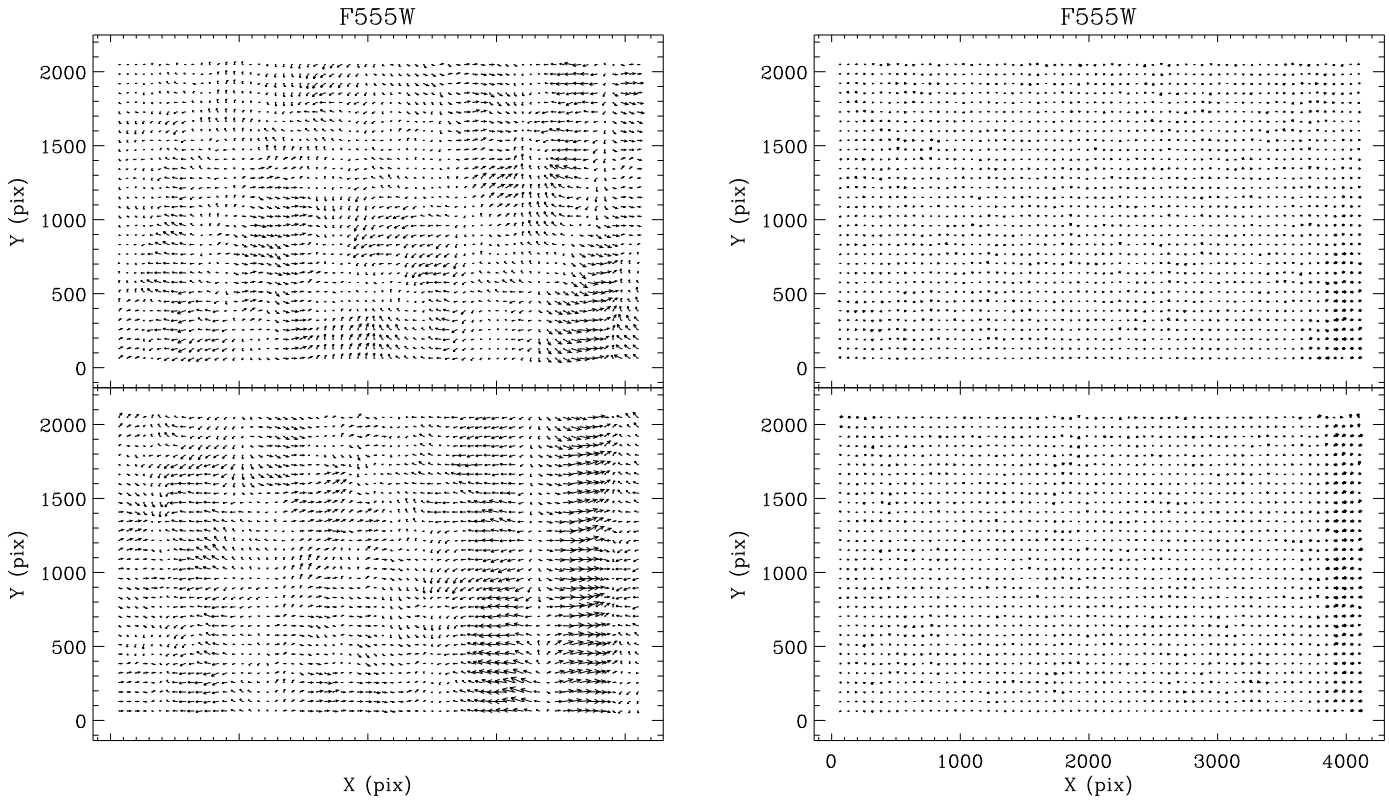

Fig. 11.— The same as in Fig.3, but for F555W UVIS filter. The largest vector before correction is ∼0.055 pixel, and 0.019 pixel after correction, both magnified by a factor of 2000. The units are WFC3/UVIS pixels.

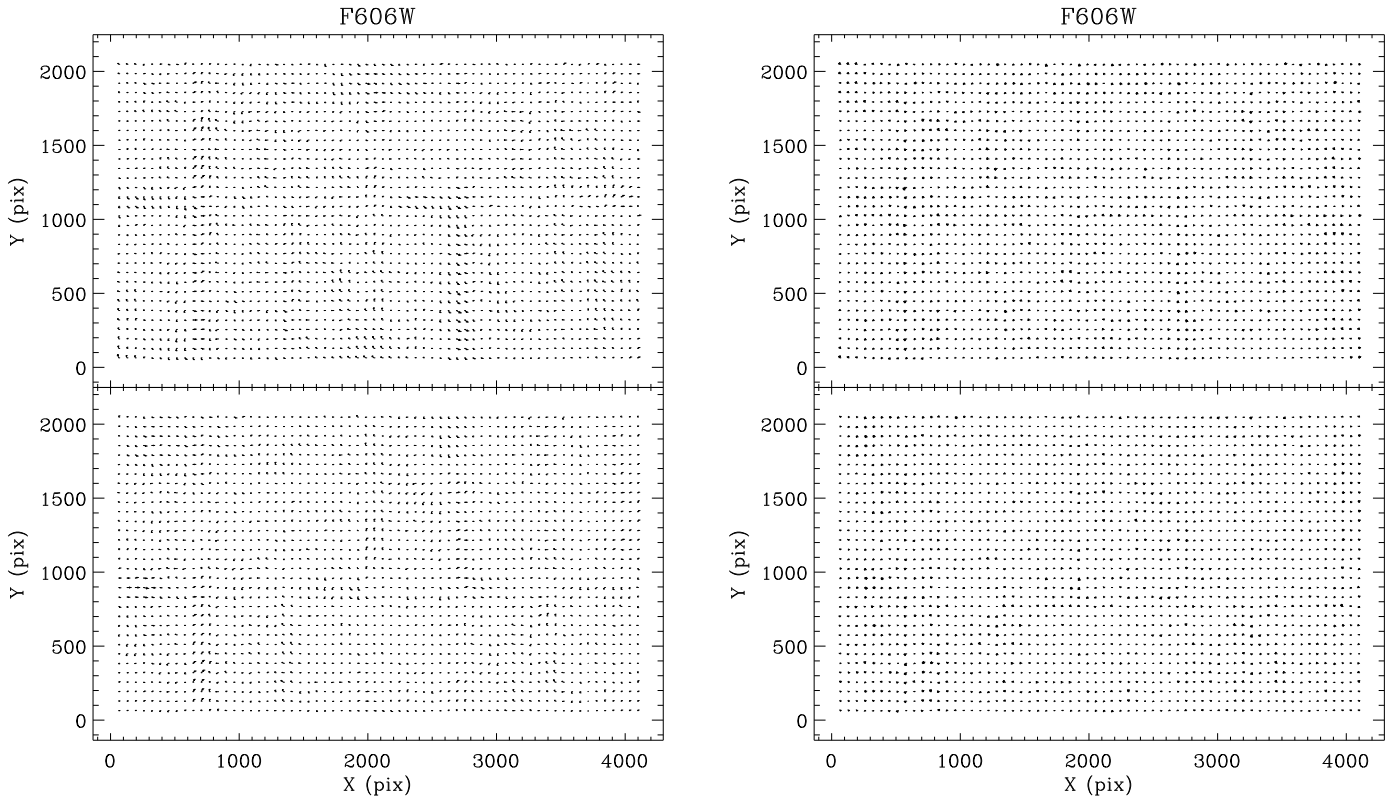

Fig. 12.— The same as in Fig.3, but for F606W UVIS filter. The largest vector is ∼0.020 pixel and 0.011 pixel, before and after the correction for filter dependent distortion, on the left and right respectively, both magnified by a factor of 2000. The units are WFC3/UVIS pixels.

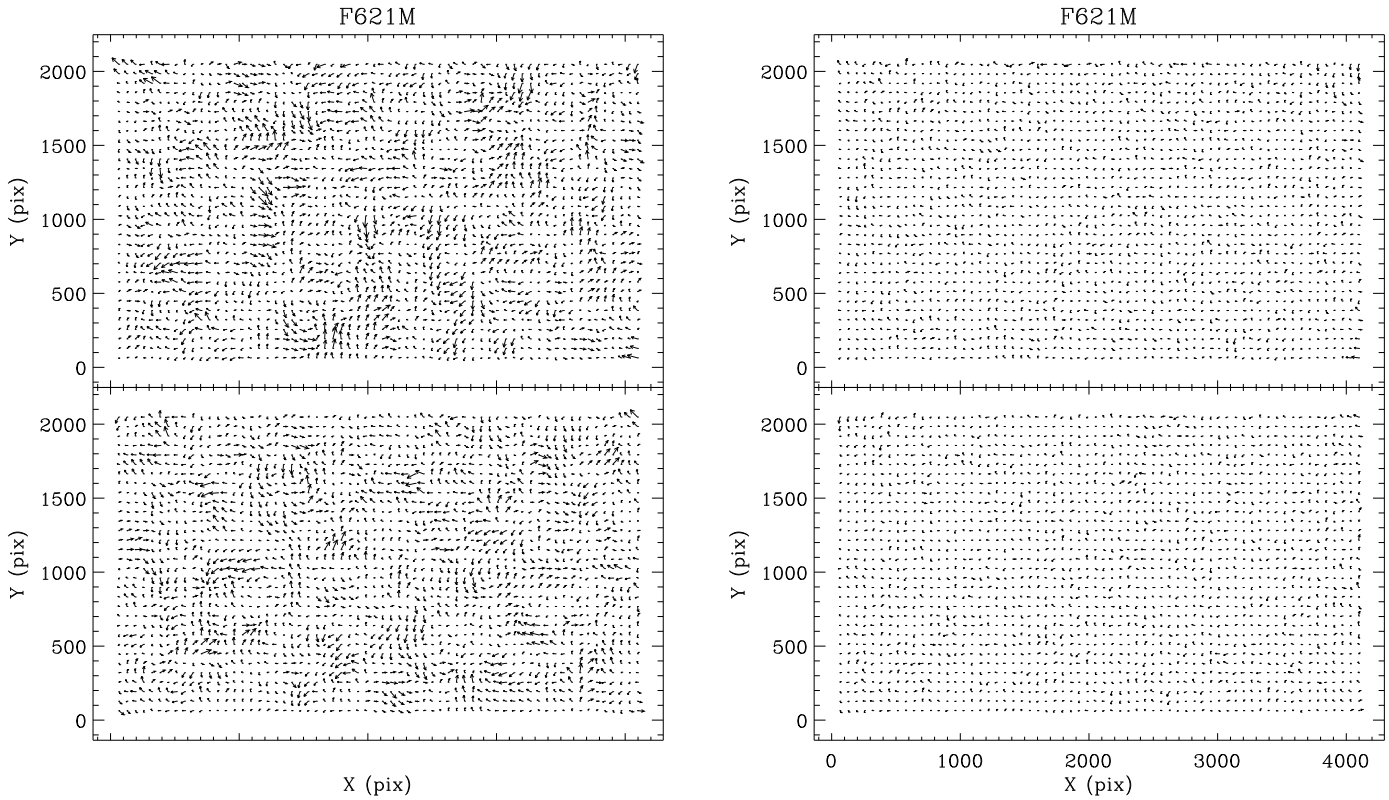

Fig. 13.— The same as in Fig.3, but for F621M UVIS filter. The largest vector is ∼0.052 pixel and 0.024 pixel, before and after the correction for filter dependent distortion, on the left and right respectively, both magnified by a factor of 2000. The units are WFC3/UVIS pixels.

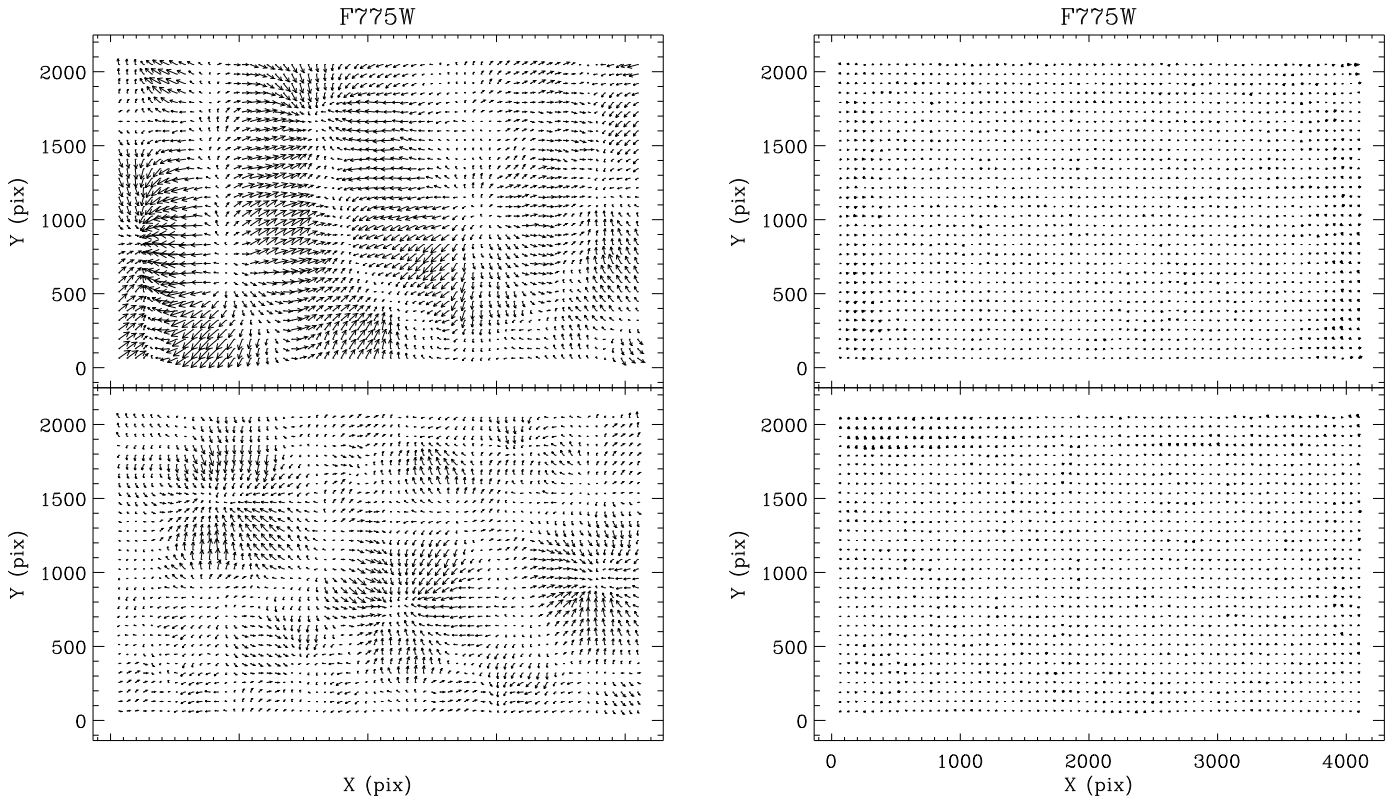

Fig. 14.— The same as in Fig.3, but for F775W UVIS filter. The largest vector before correction is ∼0.061 pixel,and 0.015 pixel after correction, both magnified by a factor of 2000. The units are WFC3/UVIS pixels.

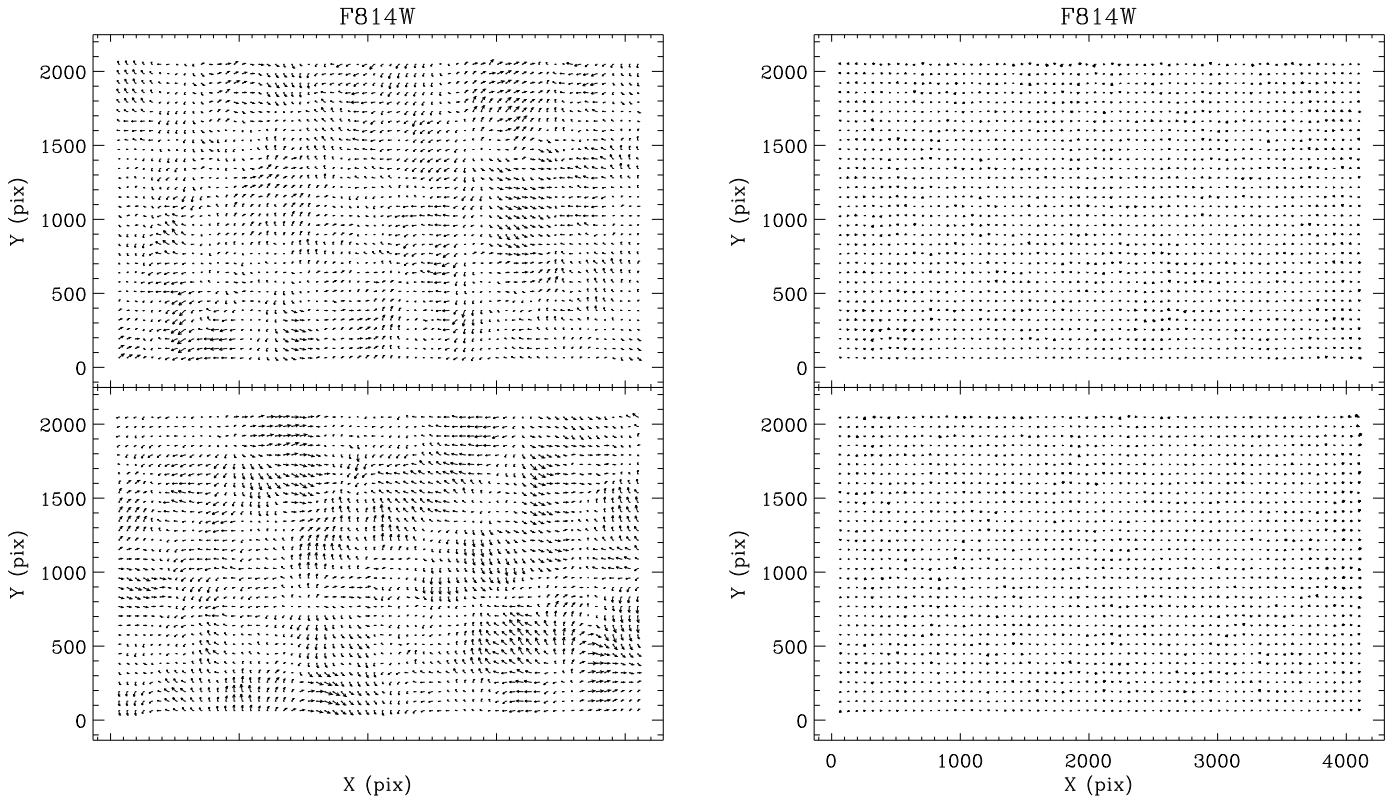

Fig. 15.— The same as in Fig.3, but for F814W UVIS filter. The largest vector is ∼0.039 pixel and 0.011 pixel, before and after the correction for filter dependent distortion, on the left and right respectively, both magnified by a factor of 2000. The units are WFC3/UVIS pixels.

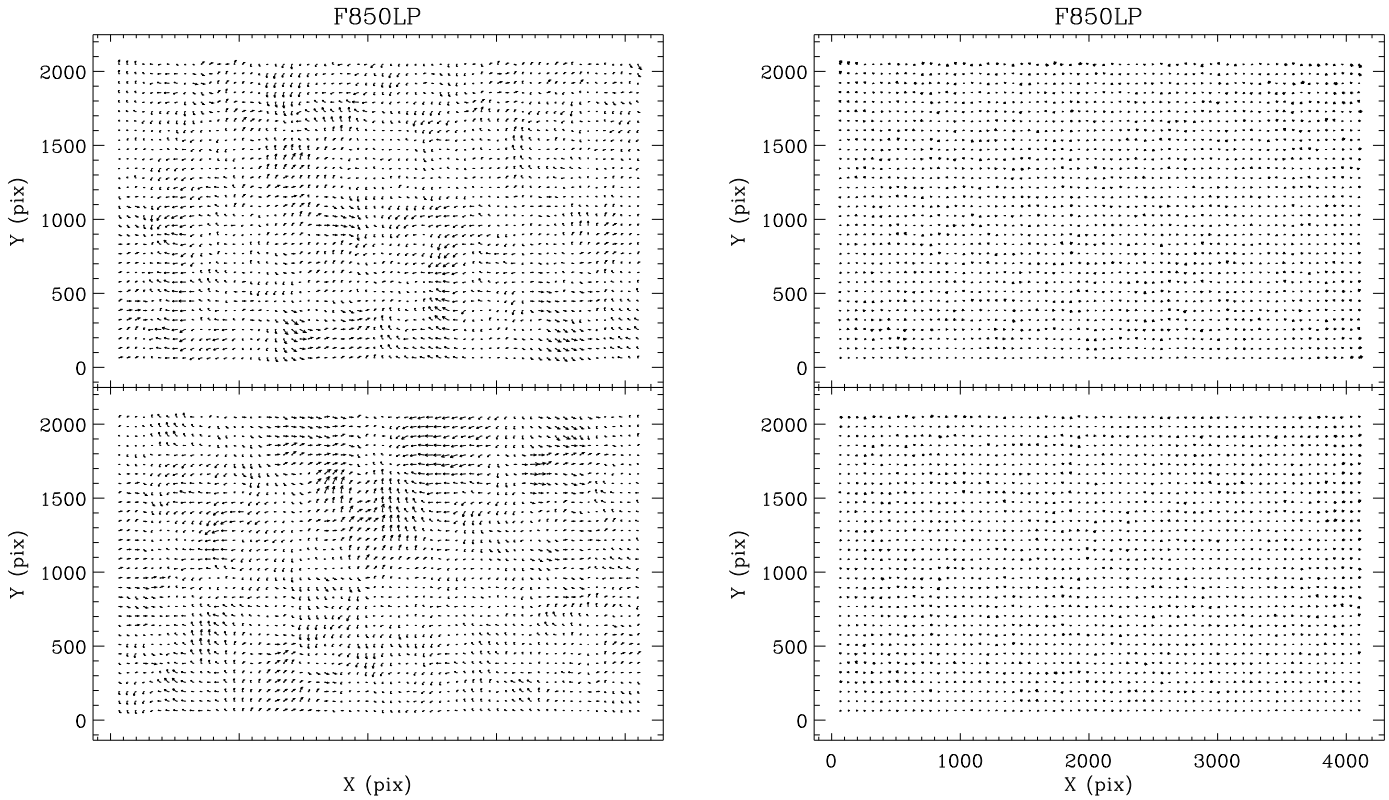

Fig. 16.— The same as in Fig.3, but for F850LP UVIS filter. The largest vector is ∼0.030 pixel and 0.016 pixel, before and after the correction for filter dependent distortion, on the left and right respectively, both magnified by a factor of 2000. The units are WFC3/UVIS pixels.

Figures 6, 7, & 10 show that not all 14 filters could be calibrated equally well, as can be seen from the enlarged amplitudes in residuals for F350LP, F390M and F475W UVIS filters. These larger irregularities can be explained by the small number of available observations (4 observations or fewer for these particular filters). For this reason, the final residuals can be reduced down to only 0.06 pixel, and the 2–D residuals maps after the correction for filter-dependent distortion look noisy.

Thus, with improved correction for the lithographic-mask pattern and filter-dependent component of distortion coupled with a better geometric distortion polynomial, the WFC3/UVIS X & Y distortion–corrected positions are accurate to $\sim$ 0.02 pixels for 11 well observed WFC3/UVIS filters. These newly derived 2–D look-up tables corrections are used for pixel-by-pixel bi-linear interpolation in WFC3/UVIS images by *DrizzlePack*/*Astrodrizzle*.

3. WFC3/UVIS Distortion Correction in STDAS software DrizzlePac

3.1. WFC3/UVIS Distortion Correction Reference Files

A main goal of newly–constructed 2–D look-up tables described above is to use them in the STSDAS software *DrizzlePack* (Gonzaga, *et al*, 2012).

As described by Hack *et al.* (2012), calibration of the distortion for HST observations is recorded and applied through the reference files, listed in the primary header of `*_flt.fits` files. The following reference files for distortion available in the header are: *i*) D2IMFILE is a reference file for the detector defect correction; *ii*) IDCTAB contains polynomial coefficients of geometric distortion; *iii*) NPOLFILE is an additional reference file for filter–dependent distortion correction.

All of these corrections are part of the World Coordinate System (WFC) transformation in the *DrizzlePack*. D2IMFILE and NPOLFILE are represented by a 2–D array that is applied to each row/column on HST images (WFPC2, ACS/WFC, WFC3/UVIS). These two 2–D look-up tables are converted into the FITS format and used in PyWCS and STWCS (Python/PyRaf) tasks.

Note that, the D2IMFILE (detector defect correction) and NPOLFILE (filter-dependent corrections) reference files , applied in *DrizzlePac*/*Astrodrizzle*/*TweakReg* software are used for pixel-by-pixel correction prior to the polynomial distortion correction.

3.2. Test with *DizzlePac* Software

The new software *DrizzlePac* (Gonzaga, *et al.*, 2012) developed recently by STSDAS has replaced the old *MultiDrizzle* software. The *DrizzlePac* software is designed to align and combine the HST images. In *DrizzlePac* there are a few tasks that can be used to perform astrometric transformations between the HST images such as a shift, rotation and

scale in order to find preliminary astrometric input for *Astrodrizzle* to align and combine HST images. One such task is *TweakReg*, an automated interface to compute the residuals, shift and rotation between HST images. This task uses, `*_flt.fits` files as input, finds X and Y positions in these images (similar to IRAF/DAOFIND), corrects X and Y positions for geometric distortion using the reference files (D2IMFILE, NPOLFILE & IDCTAB) from the header, and solves for a shift, scale and rotation between the input images (similar to IRAF task XYXYMATCH).

To test these newly derived reference files, we took a pair of ω Cen observations in each UVIS calibrated filter obtained at large HST PA_V3 roll angles ($\sim$94°). A large range of HST roll angles between two UVIS images has the advantage of overlapped UVIS1 & UVIS2, or UVIS2 & UVIS1 fields. Both UVIS CCD chip have a different pattern of systematic errors in UVIS X & Y raw positions imposed by lithographic-mask patterns and filter irregularities. Such overlapped areas between two UVIS images can serve to validate new derived correction for the lithographic-mask pattern and filter-dependent component of distortion.

Figure 17 show the residuals of X and Y positions between two F775W UVIS images taken with large HST roll angle from the output of *DrizzlePac/ TweakReg* (the plot of residuals was modified with a custom–made plotting routine). The vector residuals map (on the left panel) shows a complex structure with an amplitude of 0.1 pixel. This pattern is due to the inaccurate correction for lithographic-mask pattern and the absence of filter-dependent distortion correction. These residuals between two F775W images were derived with the old reference files as IDCTAB and D2IMFILE which are currently in the HST OPUS system. The right panel shows that once the newly–derived reference files, D2IMFILE, IDCTAB & NPOLFILE are applied, the complicated pattern of residuals is gone. It is smooth across of the entire overlapped area between two F775W images and the amplitude of residuals is reduced down to 0.02 pixel, except of the area near the edge, which can be explained by poor interpolation at the edges. Therefore, residuals of X and Y positions in the overlapping areas between two UVIS images before and after correction shows significant improvement for the fine-scale systematic.

Thus, we find that by applying the improved UVIS lithographic-mask pattern correction, and filter-dependent component of distortion correction, there is a significant improvement in the accuracy of the WFC3/UVIS distortion correction. For well measured stars in UVIS drizzled images, the *RMS* of positions residuals is now $\sim$0.02 pixel in each coordinate.

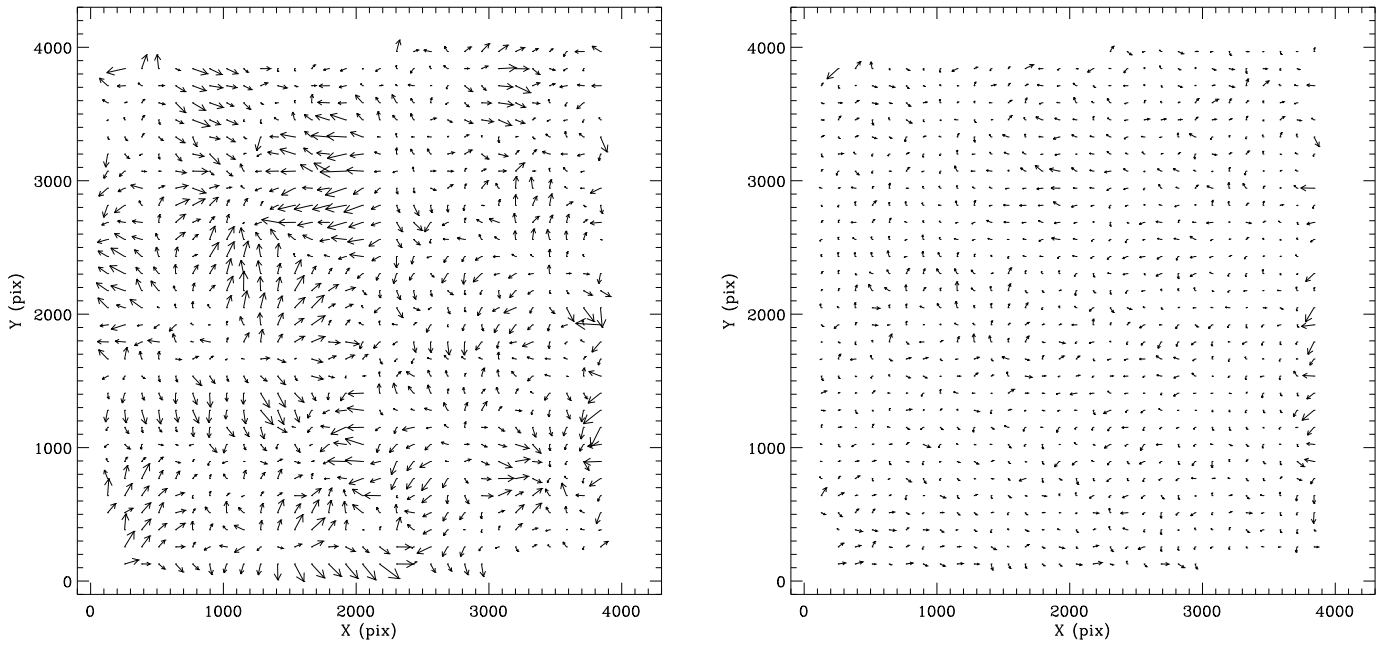

Fig. 17.— 2-D X and Y residual map between two the WFC3/UVIS images in F775W filter with large HST roll-angle as output from *DrizzlePac*/*TweakReg*. Left panel shows the residuals obtained with the old reference files while the right panel shows the residual map after applying the new improved reference files. The largest vector with old reference files is $\sim$0.08 pixel and 0.02 pixel after the correction with newly and improved reference files, both magnified by factor of 2000. The units are WFC3/UVIS drizzle pixels.

4. Conclusions

More than 4 years of observations of ω Cen in F606W UVIS filter have been used to examine and calibrate the WFC3/UVIS detector defect, related to the lithographic-mask manufacturing process. These observations have been used to construct look-up table-based corrections and remove fine-scale systematics in the X and Y positions. Then, the observations of ω Cen in 14 other WFC3/UVIS filters were used to construct a look-up tables containing filter-dependent corrections for each of the calibrated filters from CAL-11911 (PI Sabbi), CAL-12353 (PI Kozhurina-Platais), CAL-13100 (PI Kozhurina-Platais). New polynomial coefficients of geometric distortion were obtained after applying the improved lithographic-mask pattern correction and the newly–derived filter-dependent distortion. New polynomial coefficients now more accurately represent the WFC3/UVIS geometric distortion.

After applying the detector–defect correction (D2IMFILE), the newly derived filter-dependent distortion correction (NPOLFILEs), and the improved polynomial coefficients (IDCTAB), there is a significant improvement by 50-90% in the WFC3/UVIS distortion correction. The astrometric errors due to the lithographic-mask pattern and filter-dependent distortion now are $\sim$0.02 pixel for 11 well–observed UVIS filters. The fine–scale variations due to the irregularities in some UVIS filters (for example F555W and F775W) are beneficial particularly from the improvement of the large complicated structure in X and Y raw positions.

Geometric distortion in UVIS images with new improved look–up table–based correction can be corrected now at the level of 0.02 pixel ($0.8mas$). The new solution can be used in *STSDAS/DrizzlePac* for: 1) accurate stacking of WFC3/UVIS images taken with a different dither pattern and orientation; 2) rejection of CRs with higher accuracy and precision in the final drizzled UVIS images; 3) enhancement of spatial resolution; 4) deepening of the detection limit.

Further improvement of UVIS geometric distortion can be achieved by additional observations in F350LP, F390M and F475W filters and recalculating filter-dependent look-up tables. Ultimately, the accuracy level in WFC3/UVIS distortion correction mainly depends on the precision with which X and Y positions can be measured on re-sampled WFC3/UVIS images.

Acknowledgments

The fully appreciations are expressed to Jay Anderson for reviewing this ISR and for his useful comments and suggestions which improved significantly the clarity of ISR. Author also grateful to Jay Anderson for the hints using the iteration in constructing the look-up tables. V.K.-P. is greatly appreciated to John MacKenty for many valuable discussions related to the the WFC3/UVIS lithographic-mask, WFC3/UVIS filters and their properties.

References

Anderson, J., King, I., 1999, PASP, 111, 1095-1098

Anderson, J.,King, I., 2000, PASP

Anderson, J., 2002, in "2002 HST Calibration Workshop", eds S.Arribas, A. Koekemoer, B. Whitmore, (Baltimore:STScI)

Anderson, J., King, I., 2004, ACS Instrument Science Report, ACS-ISR-04-15 (Baltimore:STScI)

Anderson, J., 2007, ACS Instrument Science Report, ACS-ISR-07-08 (Baltimore:STScI)

Bellini, A., Anderson, J., Bedin, L., 2011, PASP, 123, 622-637

Golimowski, D., Sirianni, M., 2014 (private communication)

Gonzaga, S., Hack, W., Fruchter, A., et.al., 2012, "The DrizzlePac Handbook". (Baltimore: STScI)

Hack, W., Dencheva, N., Fruchter, A., Greenfield, P., 2012, Technical Sowtware Report, TSR 2012-01, (Baltimore:STScI)

Fruchter, A., Hook, P., 2002, PASP, 114, 144-152

Fruchter A., Sosey, M., et.al., 2009, " The MultiDrizzle Handbook", v.3, (Baltimore:STScI)

Koekemoer, A.,M., Fruchter, A., Hook, R.,N., Hack, W., 2002, in "2002 HST Calibration Workshop", eds A.Arribas, A. Koekemoer, B.C, Whitmore (Baltimore:STScI), p.337

Kozhurina-Platais, V., Hammer, D., Denecheva, N., Hack, W., 2013, WFC3 Instrument Science Report, WFC3-ISR-2013-14 (Baltimore:STScI)

Kozhurina-Platais, V., Borncamp, D., 2014, ACS Instrument Science Report, (in preparation)